



## OPEN ACCESS

## EDITED BY

Chen Zhao,  
Shenyang Center of China Geological  
Survey, China

## REVIEWED BY

Wei Wang,  
China University of Geosciences  
Wuhan, China  
Muhammad Irman Khalif Ahmad Aminuddin,  
Universiti Sains Malaysia Engineering  
Campus, Malaysia

## \*CORRESPONDENCE

Bishaw Mihret,  
✉ bishawmihret2022@gmail.com

RECEIVED 29 October 2024

ACCEPTED 18 March 2025

PUBLISHED 28 April 2025

## CITATION

Mihret B and Wuletaw A (2025) The  
petrography, metamorphism and deformation  
history of Neoproterozoic rock from Gida  
Ayana, Western Ethiopia: implication of  
tectonometamorphic evolution.  
*Front. Earth Sci.* 13:1519116.  
doi: 10.3389/feart.2025.1519116

## COPYRIGHT

© 2025 Mihret and Wuletaw. This is an  
open-access article distributed under the  
terms of the [Creative Commons Attribution  
License \(CC BY\)](https://creativecommons.org/licenses/by/4.0/). The use, distribution or  
reproduction in other forums is permitted,  
provided the original author(s) and the  
copyright owner(s) are credited and that the  
original publication in this journal is cited, in  
accordance with accepted academic practice.  
No use, distribution or reproduction is  
permitted which does not comply with  
these terms.

# The petrography, metamorphism and deformation history of Neoproterozoic rock from Gida Ayana, Western Ethiopia: implication of tectonometamorphic evolution

Bishaw Mihret<sup>1\*</sup> and Ajobush Wuletaw<sup>2</sup>

<sup>1</sup>Structural Geology & Tectonics, Natural and Computational Science, Debre Markos University, Debre Markos, Ethiopia, <sup>2</sup>Economic Geology, Natural and Computational Science, Debre Markos University, Debre Markos, Ethiopia

The geological study of basement rocks in the Gida Ayana area of western Ethiopia has revealed significant findings regarding the local petrography, metamorphism, and deformation history. The geological evolution of rocks in the area has been analyzed thoroughly through detailed field investigations, overprinting and cross-cutting relationships, and petrographic studies of metamorphic rocks. The findings reveal that the study area experienced polyphase deformations, with at least three ductile deformation phases (D1 to D3) associated with two metamorphic events (M1 and M2), and development of brittle structures such as irregular fractures, joints, and veins. Each type of structure observed in the study area has been discussed in detail, highlighting the formation of F2 folds, S2 foliations, L2 lineations, S3 foliations, F3 folds, and joints. The development of a steep northeast-to-southwest striking foliation S2 gneissic banding and mineral assemblage (Or + Pl + Qtz + Bt + - Sp) indicate that the prograde metamorphism (M1) is synchronous with D2 phase. The alteration products sericite, chlorite, and biotite indicate a retrograde metamorphism (M2) that may have occurred during uplift or D3 shear-zone-related fluid migrations. The regional tectonic setting of Gida Ayana is within the East African Orogen. The relationships between the Gida Ayana metamorphism and deformations with larger tectonic processes, such as continental collisions during the pan-African Orogeny, were discovered. We also analyzed the orientation and features of the deformation structures as well as their associated metamorphic events to offer important insights into the tectonic and metamorphic history of the East African Orogen.

## KEYWORDS

deformation history, Gida Ayana, metamorphic event, metamorphism, petrography

## 1 Introduction

The Precambrian basement, Late Paleozoic to Early Tertiary sediments, and Cenozoic volcanic and related sedimentary rocks comprise the three primary geological formations of Ethiopia (Tefera and Hara, 1996). The Precambrian era produced the basement rocks

that are the oldest in the nation and range in age from 600 to 3,000 million years. These rocks comprise various metamorphically altered lithological types, including schists, gneisses, phyllite, quartzite, granitoid, mafic, and ultramafic types. These Precambrian rocks are associated with the Paleozoic Mozambique belt and pan-African orogenic event (Kazmin et al., 1978). The Precambrian rocks of Ethiopia are exposed in the peripheral regions of the country, including the north, west, southwest, south, and east (Asrat et al., 2001). These rocks are found in areas less affected by Cenozoic volcanism and rifting where the Phanerozoic cover rocks have eroded (Tefera and Hara, 1996). In Ethiopia, the Precambrian rocks include the Arabian Nubian Shield (ANS) in the north and gneissic rocks of the Mozambique Belt (MB) in the south (Ayalew, 1997). These terranes exhibit distinct lithotectonics with different lithological associations, internal structures, and metamorphic grades.

The ANS includes low-to medium-grade metamorphic rocks, while the MB comprises high-grade reworked rocks that constitute the Western Ethiopian Precambrian Shield (Kazmin et al., 1978). Yubdo Daltti to Tulu Dimtu range is home to linear bands of ultramafic rocks, volcano-sedimentary greenschist assemblages, and high-grade gneisses that comprise the crystalline basement of western Ethiopia. The basement rocks are penetrated by plutonic rocks of different ages and compositions (Yihunie and Hailu, 2007). A portion of the Neoproterozoic rocks dating from approximately 750 million years ago are exposed in the western Ethiopian Precambrian shield (Allen et al., 2005; Gani and Abdelsalam, 2006). Among these rocks, the Gida Ayana Precambrian rocks are known for their unique mineral composition and geochemical signatures. These rocks have been subjected to intense deformation and metamorphism, resulting in a complex assemblage of minerals and structures. The main objective of this study is to provide a comprehensive understanding of the petrography, metamorphism, and deformation history of the Neoproterozoic rocks in Gida Ayana by integrating fieldwork, petrographic analysis, and structural geological interpretation; this work is aimed at reconstructing the tectonometamorphic evolution of the region by providing new insights into the East African Orogeny (EAO) and its implications on the regional geology.

## 2 Description of the study area

The study area is located in the western part of Ethiopia in the Oromia regional state, specifically to the south of Gida Ayana town (Figure 1). The geographical coordinates of the study area are 231304–284444 easting and 1091655–1109742 northing. This area can be accessed through the main road by first traveling from Addis Ababa to Nekemete (distance of 315 km) and then turning toward Gida Ayana town (distance of 114 km). There are also numerous networked and motorable dry-weather foot trails that allow good traversal during geological mapping.

## 3 Methodology

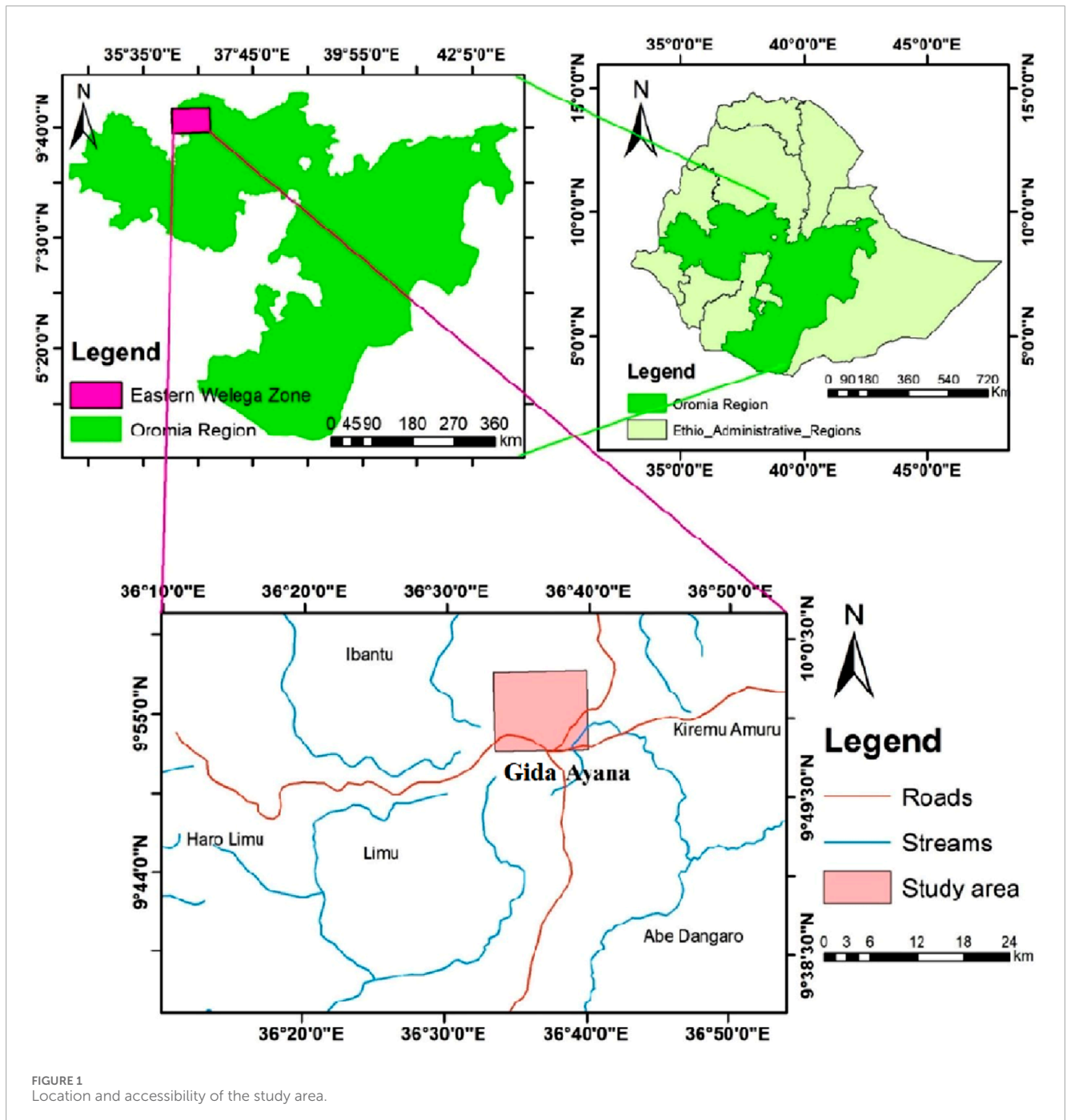
Several analytical techniques were employed to achieve the objective of this study, including fieldwork, petrographic analysis,

and deformation analysis. The fieldwork was conducted between March and June 2023 as well as in early 2024 briefly, which involved foot traverses lasting 1–8 d. The focus was on geological mapping of the Gida Ayana region to identify the lithological units, structural features, and geological contacts as well as to collect rock samples. These samples were chosen based on the geological context by emphasizing key lithological units that could provide insights into the metamorphic and deformation history of the area. Petrographic analysis was performed using optical microscopy with thin sections prepared from representative rock samples to examine the mineralogy, texture, and grain size; this analysis allowed the identification of minerals such as quartz, feldspar, mica, garnet, and sillimanite, along with observations on the degree of metamorphism based on textural features like foliation, lineation, and presence of deformed minerals. Additionally, macroscopic structural analysis was conducted in the field to investigate deformation features, such as joints, folds, and shear zones, followed by geometrical analysis to quantify the orientations, shapes, and strains. On the microscopic scale, the deformation microstructures were analyzed to understand the strain history and mechanisms by focusing on grain boundary migration, dynamic recrystallization, and cataclasis. Strain quantification was performed using methods like strain ellipsoids and focal mechanism analysis aided by structural geology software such as Stereonet, Rose diagram plotter, and RockWare for 3D modeling and structural data analyses. These techniques allowed for a comprehensive understanding of the metamorphic, deformation, and petrological history of the Gida Ayana region.

## 4 Regional geology

The EAO is a significant orogenic belt extending approximately 6,000 km along the eastern flank of Africa that was formed by the collision of East and West Gondwana during the late Proterozoic era (Stern et al., 2012). The tectonic evolution of the EAO includes Rodinia rifting, continent–continent collisions, and crustal shortening, leading to the formation of northwest–southeast faults (Stern, 1994). The evolution of the EAO is a result of a Neoproterozoic to lower Paleozoic Wilson cycle (Kusky et al., 2003; Li et al., 2008). The ANS in northeast Africa and western Arabia is the largest tract of juvenile Neoproterozoic crust affected by the pan-African orogenic cycle (Abdelsalam and Stern, 1996); it is characterized by juvenile nature, low-grade metamorphism, and abundant island-arc rocks and ophiolites (Kroner and Stern, 2004; Tsige and Abdelsalam, 2005). It was formed through a multistage process of colliding and coalescing juvenile terranes. The ANS underwent two major tectonic–metamorphic phases approximately 750 Ma and 700 Ma, leading to the formation of tight north–south-trending upright folds (Johnson and Woldehaimanot, 2003; Avigad et al., 2007).

The ANS is composed of extensive low-grade Neoproterozoic volcano-sedimentary sequences with associated dismembered ophiolites aligned along the suture zones (Berhe, 1990; Braathen et al., 2001). It also includes supracrustal metavolcanic metamorphoses in the greenschist facies and is intruded upon by granites and gabbro dikes (Avigad et al., 2007). In Ethiopia, the ANS is intertwined with the MB, which experienced intense collisions between the East and West Gondwana fragments



(Stern, 1994). The ANS is exposed at the upper-to-middle crustal levels and contains abundant ophiolites as well as subduction- or collision-related granitoids that distinguish it from the MB (Ayalew et al., 1990; Abdelsalam and Stern, 1996).

The MB defines the southern part of the EAO and consists of medium-to-high-grade gneisses and voluminous granitoids (Kroner and Stern, 2004). It extends from the ANS into southern Ethiopia, Kenya, Somalia, Tanzania, Malawi, Mozambique, and Madagascar. The collision between East and West Gondwana led to the formation of the pan-African EAO, resulting in a pan-African collage of terranes accreted to the eastern margin of the Congo and Tanzania cratons (Kroner and Stern, 2004). These tectonic events also

resulted in closure of an oceanic basin approximately 760 Ma and the formation of major north-trending transcurrent faults at approximately 635 Ma (Abdelsalam and Stern, 1996; Asrat and Barbey, 2003). The MB rocks are well-exposed in various regions of east Africa, including Kenya, Ethiopia, Somalia, and Madagascar (Kazmin et al., 1978; Alemu and Abebe, 2007).

The Ethiopian Precambrian rocks are found in various parts of the country and comprise a diverse range of volcano-sedimentary and plutonic rocks that have undergone varying degrees of metamorphism (Asrat et al., 2001) (Figure 2A). They range in age from 880 to 550 million years and form the crustal backbone of the Ethiopian region (Abbate et al., 2015). The Western Ethiopian Shield

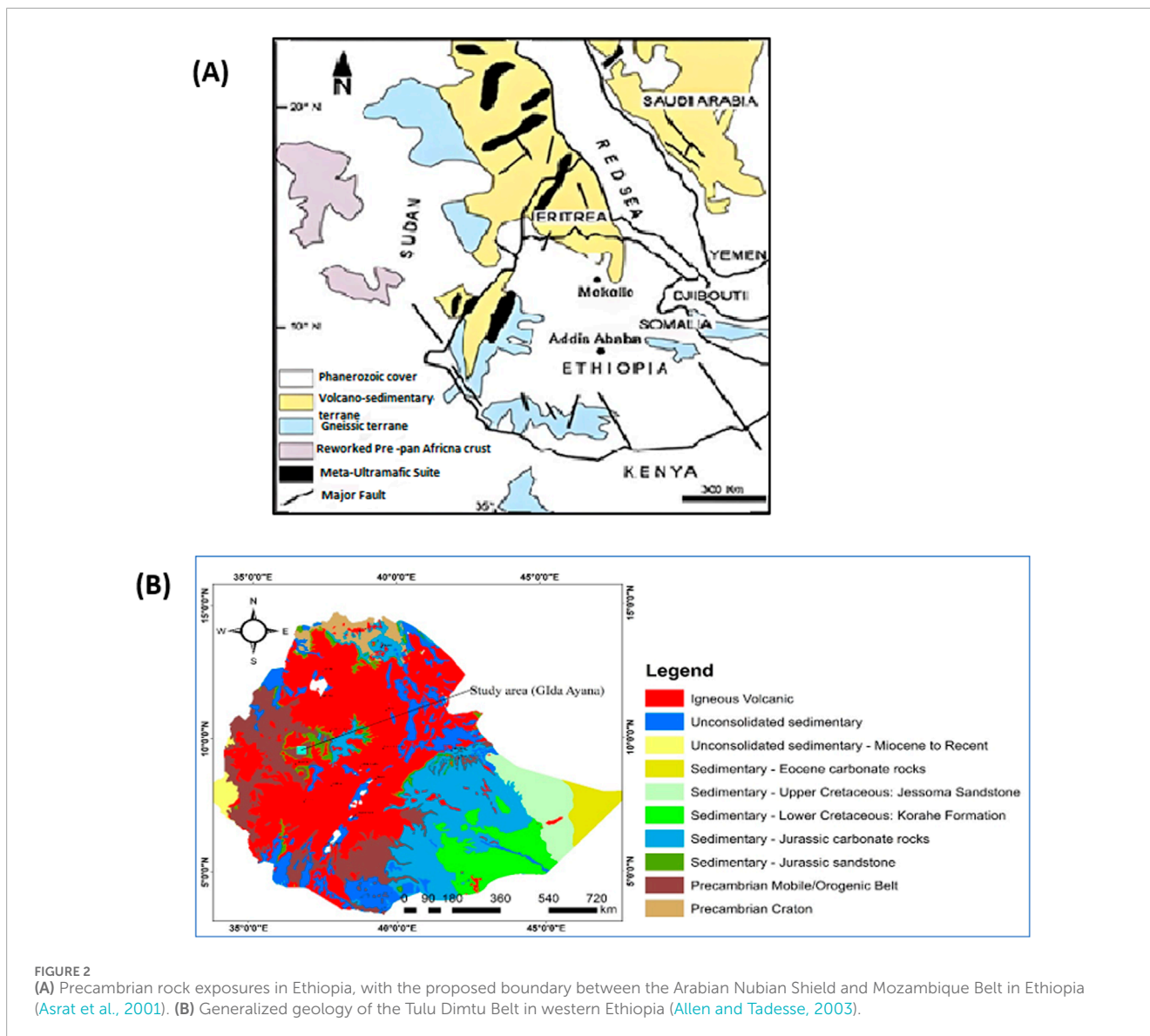


FIGURE 2 (A) Precambrian rock exposures in Ethiopia, with the proposed boundary between the Arabian Nubian Shield and Mozambique Belt in Ethiopia (Asrat et al., 2001). (B) Generalized geology of the Tulu Dimtu Belt in western Ethiopia (Allen and Tadesse, 2003).

(WES) comprises low-to-medium-grade metamorphic rocks of the ANS and high-grade reworked rocks of the MB (Braathen et al., 2001; Allen and Tadesse, 2003) (Figure 2B). The Precambrian rocks in this region include high-grade gneiss and migmatite as well as low-grade meta-volcano-sedimentary rocks, whose ages range from approximately 830 to 540 million years according to geochronological investigations (Abbate et al., 2015). These rocks are correlated with the juvenile pan-African assemblages of northern Ethiopia, Eritrea, and southeastern Sudan (Alemu and Abebe, 2007). The western Ethiopian Precambrian shields are subdivided into several domains, including the Birbir, Geba, and Baro domains (Ayalew and Peccerillo, 1998; Ayalew and Johnson, 2002; Allen and Tadesse, 2003).

The Birbir domain is characterized by deformed and metamorphosed volcano-sedimentary rocks along with ultramafic-to-felsic magmatic rocks (Johnson et al., 2004); it is bound by the Geba and Baro domains. Additionally, it includes metasedimentary rocks, metavolcanics, subvolcanic sills, dykes, and mylonitic quartz diorite (Ayalew and Johnson, 2002). The Baro and Geba domains in

the eastern and western parts of the western Ethiopian Precambrian shield comprise quartzofeldspathic gneisses, biotite and hornblende-biotite gneisses, and migmatitic rocks (Ayalew and Johnson, 2002). The Baro domain also contains paragneiss near its eastern margin (Allen and Tadesse, 2003). The Didessa domain located east of the Didessa River in the Wollega area consists of medium-grade paragneisses and orthogneisses with banded mafic gneiss; it is differentiated from the adjacent Kemashi domain by distinct lithological and structural characteristics. The Kemashi domain parallel to the Tulu Dimtu belt comprises sequences of metasedimentary rocks of marine origin, mafic to ultramafic metavolcanic rocks, and associated plutonic rocks. The Dengi domain includes deformed and metamorphosed volcano-sedimentary sequences, coarse-grained paragneissic and orthogneissic units, and mafic-to-felsic intrusive bodies, all of which indicate two pulses of magmatism approximately 850–840 Ma and 780–760 Ma (Blades et al., 2015). The Sirkole domain is located west of Assosa town and extends into Sudan with unknown western limits. It consists of north–south elongated blocks with alternating sequences of moderate-grade polydeformed and metamorphosed

gneisses, low-to-moderate-grade metasedimentary rocks, and mafic-to-felsic metavolcanic rocks intruded upon by granitoid plutons. The Daka domain encompasses gneissic rocks and includes a banded orthopyroxene-bearing granulite facies unit known as Daka gneiss.

The WES has an area of approximately 650 km<sup>2</sup> and is the largest Precambrian block in Ethiopia (Abdelsalam and Stern, 1996; Alemu and Abebe, 2007); it evolved through different processes, including early rifting, subduction, island-arc formation, arc accretion, and continent–continent collision (Kazmin et al., 1978; Stern, 1994). Intrusive bodies within the WES have a wide compositional spectrum from gabbro to granite and are categorized as pre- to post-deformation granitoids within the plate and volcanic arc settings (Grenne et al., 1998; Ayalew and Johnson, 2002; Kebede and Koerber, 2003). Metamorphism in the WES occurred in a wide range of grades from low to very high (Ayalew and Peccerillo, 1998).

## 5 Results and discussion

### 5.1 Geology and petrography of the Gida Ayana area

The study area is a part of the high-grade metamorphic terrane of the WES that is dominated by both Precambrian high-grade metamorphic and intrusive rocks (Figure 3). The high-grade metamorphic rock is represented by migmatitic gneiss (orthogneiss comprising hornblende–biotite gneiss and granitic gneiss) that is exposed in the eastern, central, southeastern, and southwestern parts of the study area, whereas the Precambrian intrusive rock is represented by granite that is exposed in the western, northwestern, and southwestern parts of the study area. Both rock units cover the largest portion of the study area. The orthogneiss rocks are relatively foliated and banded. Most of the rocks in the study area are affected by secondary structures like joints, fractures, quartz veins, and faults as well as generally exposed to a relatively low-lying and rugged topography. The following description provides an account of the geology of the rocks in the study area, i.e., rock type, including the mineralogy in modal composition shown in Table 1 and texture.

#### 5.1.1 Quartz–feldspar migmatite

This unit is extensively exposed on the northeastern side of the study area (Figure 3) and has a gradational contact with the adjacent lithologic unit. It shows weathered color variation from light gray to dark brown and fresh coloration from pinkish to dark color (Figure 4A). The outcrops and hand specimens are coarse-grained and composed of quartz, feldspar, and varying proportions of mafic minerals (especially biotite) and hornblende. Occasionally, gneissic banding is visible but is generally discontinuous, partly assimilated, and obliterated by granitic materials, which result from *in situ* melting and granitization. The discontinuous foliations are mainly north–south striking. However, the orientation of the major foliation is sometimes difficult to measure because it is highly stigmatized, and the compositional layers are contorted, irregularly oriented, and pygmatally flow-folded.

Thin-section analysis of this rock unit indicates that it is coarse-grained with well-preserved granoblastic textures (Figures 4B,C). It is mainly composed of plagioclase, hornblende, orthoclase, biotite, and quartz. Accessory minerals like sphene, pyroxene, hornblende,

and opaque iron-oxide minerals are also found in some of the samples. In addition, epidote, sericite, and muscovite occur as newly formed retrograde minerals. The modal analysis of the samples shows that this unit is composed of 35% orthoclase, 30% plagioclase, 16% microcline, 16% quartz, 1% hornblende, and 1% biotite, with the remaining portion composed of accessory minerals like sphene, opaque minerals, and apatite.

#### 5.1.2 Amphibole gneiss

This rock unit is exposed mainly in the northwestern and southwestern parts of the mapped area (Figure 3), mostly weathered, friable, gneissose, and coarse-grained, with an alternating dark-green highly foliated (very mafic rich, e.g., hornblende and biotite) to light-grayish (felsic rich, e.g., plagioclase and quartz) band (Figure 4D). Alteration of minerals such as biotite, epidote, and chlorite are common given the retrograde metamorphic alteration of hornblende along the shear zone. This rock unit mostly occurs in highly jointed, fractured, and veined forms, with majorly N10°E to N20°W strikes and westerly dips.

Petrographically, thin sections of this unit are composed of medium-grained, mostly equigranular, short-to-medium prismatic hornblende, plagioclase, alkali feldspar, and quartz (Figures 4E,F). Texturally, the rock exhibits a porphyroblastic texture and contains large crystals of plagioclase and alkali feldspars. The plagioclase porphyroblast contains fine-grained low-grade minerals such as albite, actinolite, quartz, epidote, and small grains of opaque minerals as inclusions. The mineralogical composition of the rock is 50% hornblende, 20% quartz, 15% plagioclase, 10% clinopyroxene, 5% biotite, and trace opaque minerals. These minerals define a porphyroblastic and perthitic texture. The alteration is not intense, but those observed include minor phases of sericite after plagioclase and epidote after hornblende.

#### 5.1.3 Hornblende gneiss

This rock unit typically appears dark-to-medium gray and slightly greenish depending on the amount of hornblende and other minerals present (Figure 5A). The most distinctive feature of hornblende gneiss in the field is its foliation or banding, which can range from fine to coarse owing to the alignment of minerals in layers or bands, giving it a striped appearance. The principal minerals in hornblende gneiss include hornblende (amphibole group), plagioclase feldspar, quartz, biotite mica, and sometimes even trace amounts of minerals like chlorite, apatite, or epidote (Figures 5B,C). Hornblende is often the most prominent mineral in this rock type, as suggested by its name. In a petrographic description, more detailed analysis using a microscope provides insights into the mineral composition and structure at the microscopic scale. The hornblende gneiss is composed of 60% hornblende, 25% quartz, 10% orthoclase, and 4% epidote, along with accessory epidote (green), chlorite, and sphene.

#### 5.1.4 Biotite–hornblende gneiss

This rock unit is dominantly exposed in the central and sometimes in the southeastern parts of the study area (Figure 3). It has medium-to-coarse grain size, a dark gray color when freshly exposed, and light-to-greenish gray when weathered (Figure 5D). It exhibits a foliated fabric and is primarily made up of minerals such as plagioclase, hornblende, and biotite. These minerals are flaky and oriented differently, resulting

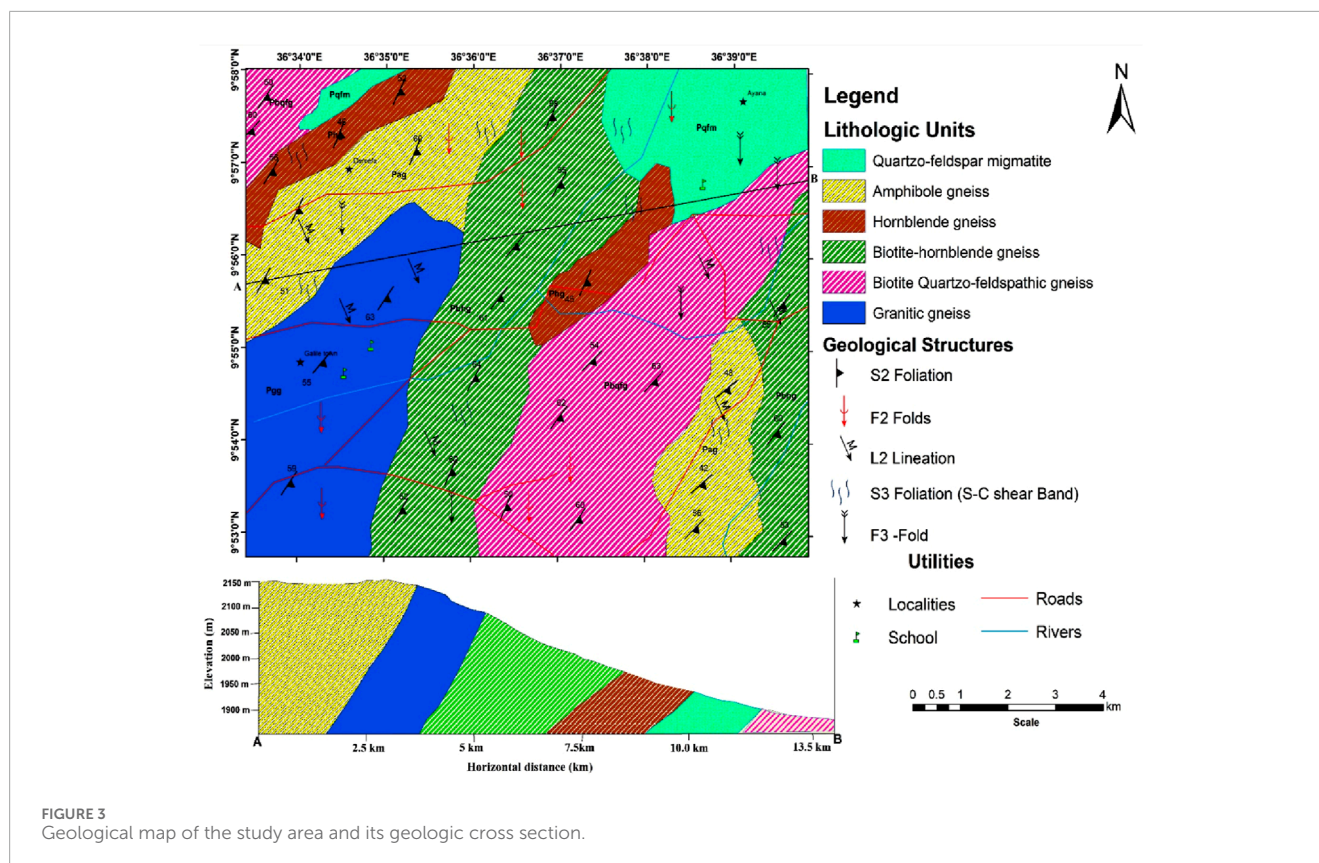


FIGURE 3  
Geological map of the study area and its geologic cross section.

in a gneissose structure (Figure 5D). The compositional variations with segregation of mafic and felsic minerals are likely formed through differentiation during high-grade metamorphism. The rock shows mesoscale fabric with N15°E to S18°W strike and mostly easterly dip with a slight westerly dip, along with foliations intersected by quartz veins. It is highly fractured and sheared in some areas and is typically found in low-lying rugged terrain.

Petrographic analysis reveals varying mineral compositions in different samples (Figures 5E,F). The biotite–hornblende gneiss is a dark-gray fine- to medium-grained rock composed of 30% quartz, 30% plagioclase, 20% hornblende, 12% biotite, and 5% epidote. Microcline, opaques, orthoclase, sphene, and sericite are also found in minor amounts, whereas apatite and calcite are found in trace amounts. The petrographic study further reveals that the quartz grains are strongly milled and ribboned, probably along the local shear zones.

### 5.1.5 Biotite quartzofeldspathic gneiss

This type is mainly found in the eastern, central, and some northwestern regions of the study area, along with amphibole and biotite hornblende gneiss rocks (Figure 3). It has a light gray color when weathered and is whitish to light pink when fresh, with a medium-to-coarse-grained texture containing flaky minerals like biotite (Figure 6A). It is primarily composed of quartz, feldspar, biotite, and plagioclase and exhibits segregation of mafic and felsic minerals; the rock also exhibits sericitization and chlorination alterations with signs of fracturing, weathering, and local alterations. The foliation orientation is N35°E with dips of 65°NW

in the contrast lithologies, which indicate that the unit may have had a tectonic contact.

Petrographic analysis reveals that the quartzofeldspathic gneiss is composed of 40% plagioclase (andesine), 25% quartz, 15% biotite, 10% orthoclase, and 5% microcline, with minor amounts of muscovite, chlorite, sericite, calcite, sillimanite, and opaques (Figures 6B,C). Here, the plagioclase is altered to white mica and calcite, while the porphyroclasts of quartz and feldspar are enveloped by fine matrices of the same minerals. A few feldspars are shattered and are often replaced by secondary white mica along twin lamellae and cleavage traces. The biotite component is greenish owing to incipient chlorination.

### 5.1.6 Granitic gneiss

The granitic gneiss only occurs in the southwestern part of the study area (Figure 3) and is generally exposed in a relatively low-lying and rugged topography along the river gorges. This unit has gradational contact with the surrounding rock unit. The texture of the granitic gneiss is typically foliated, meaning that it exhibits a banded or layered structure owing to the alignment of minerals under directed pressure. The banding can vary in intensity, ranging from subtle to pronounced, depending on the degree of metamorphism and the original composition of the granite protolith. The granitic gneiss is commonly pinkish on the fresh outcrop, medium-to-coarse-grained (fine-grained varieties occur very rarely when strongly deformed or sheared), and gneissose (Figure 6D), exhibiting textural and mineralogical homogeneity.

Petrographically, thin sections of the rock are medium-to-coarse-grained and mainly composed of k-feldspar (up to 43%),

TABLE 1 Modal percentages of the representative rock samples.

Sample name	Mineral name and their modal (%)												Coordinate location
	Qtz	Kfs	Plag	Ms/Ser	Bt	Opq	Zr	Pyr	Spn	Chl	Hbl	Apt	
BH-01	25	25	20	10	12	2	-	-	-	5	10	3	E: 250000, N: 1095000
BU-02	20	10	25	15	10	2	-	-	-	5	10	2	E: 265000, N: 1098000
BH-03	25	10	20	10	20	1	1	-	-	10	7	1	E: 275000, N: 1099500
BH-04	25	30	10	5	20	3	-	-	-	7	25	1	E: 231304, N: 1091655
BH-05	30	15	25	5	25	1	1	-	-	5	3	1	E: 284444, N: 1097000
BH-06	30	15	25	5	10	1	-	-	-	4	10	-	E: 245000, N: 1101000
BH-07	20	10	25	5	20	-	-	-	-	10	30	-	E: 260000, N: 1105000
BH-08	20	5	15	5	25	1	-	-	-	12	35	-	E: 270000, N: 1102000
BH-09	20	-	25	-	8	1	-	3	-	3	40	-	E: 240000, N: 1098500
BH-10	30	40	15	-	10	2	-	-	2	-	-	-	E: 255000, N: 1105000
BH-11	35	45	10	2	5	2	-	-	-	2	-	1	E: 236000, N: 1097000
BH-12	30	45	14	3	5	2	1	-	-	-	-	-	E: 265500, N: 1100000
AB-13	15	-	30	-	5	2	-	5	4	-	35	1	E: 250500, N: 1108000
BH-14	20	-	25	-	10	2	-	5	4	-	38	1	E: 278000, N: 1106000

Note: Qtz = quartz, Kfs = potassium feldspar, Plag = plagioclase, Ms/Ser = muscovite/sericite, Bt = biotite, Chl = chlorite, Hbl = hornblende, Apt = apatite, Opq = opaque mineral, Zr = zircon, Pyr = Pyrite, Spn = sphene, E = Easting coordinate, N = northing coordinate.

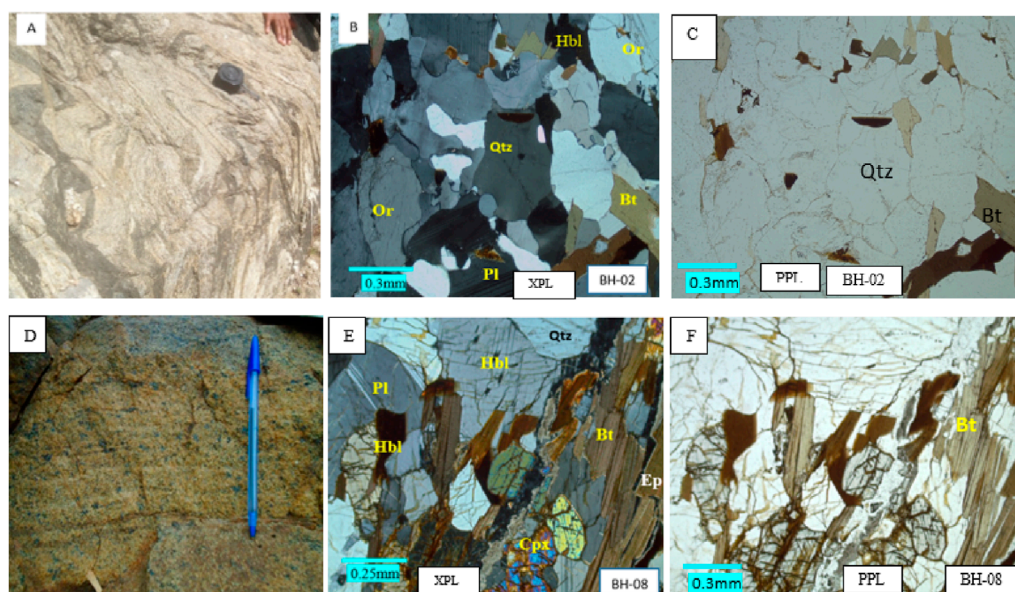
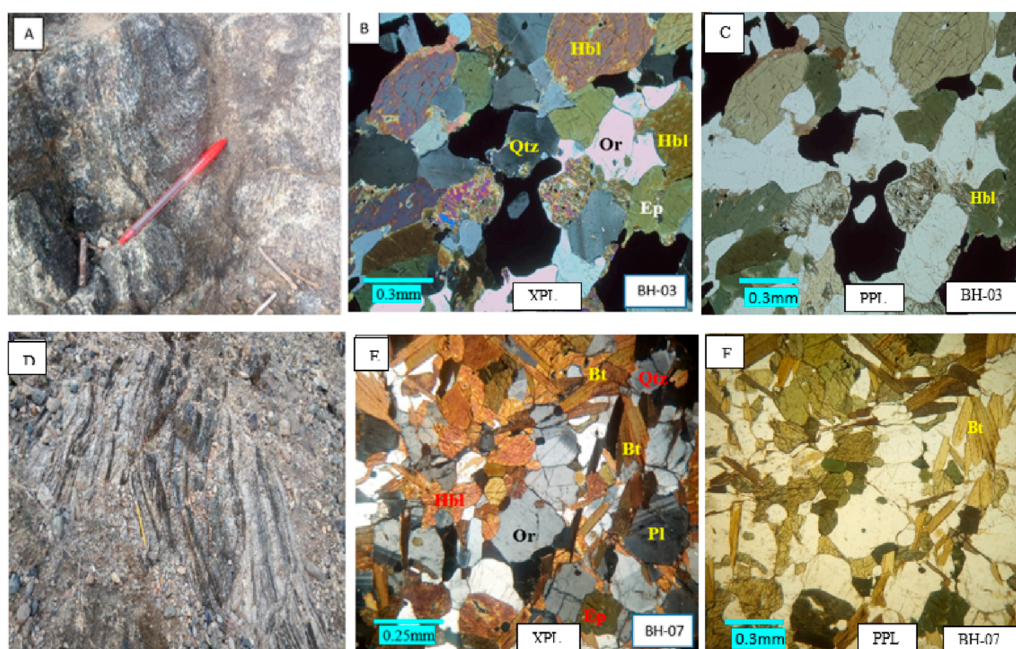
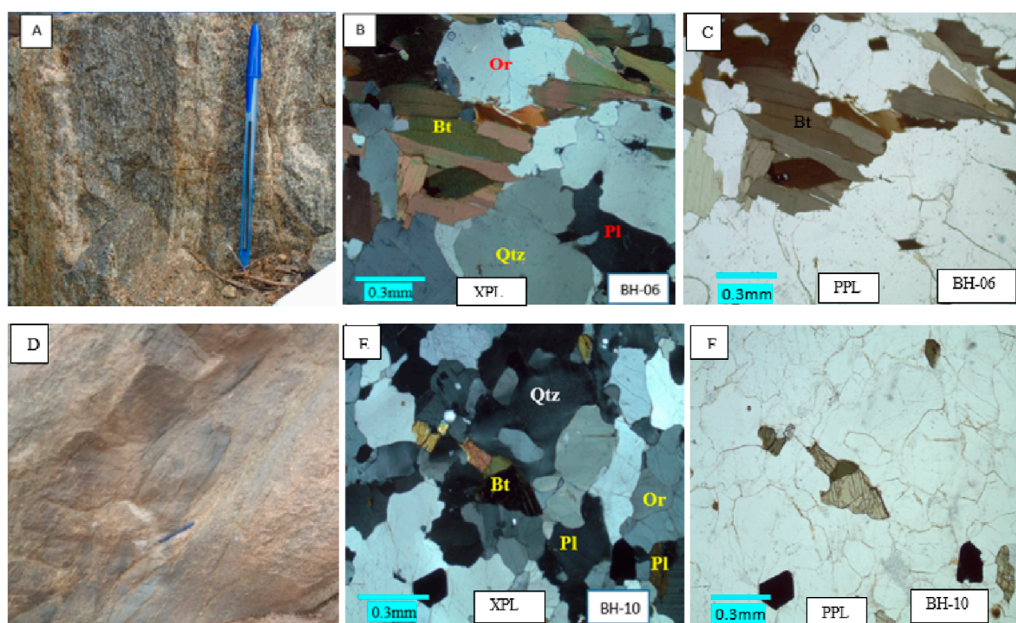


FIGURE 4

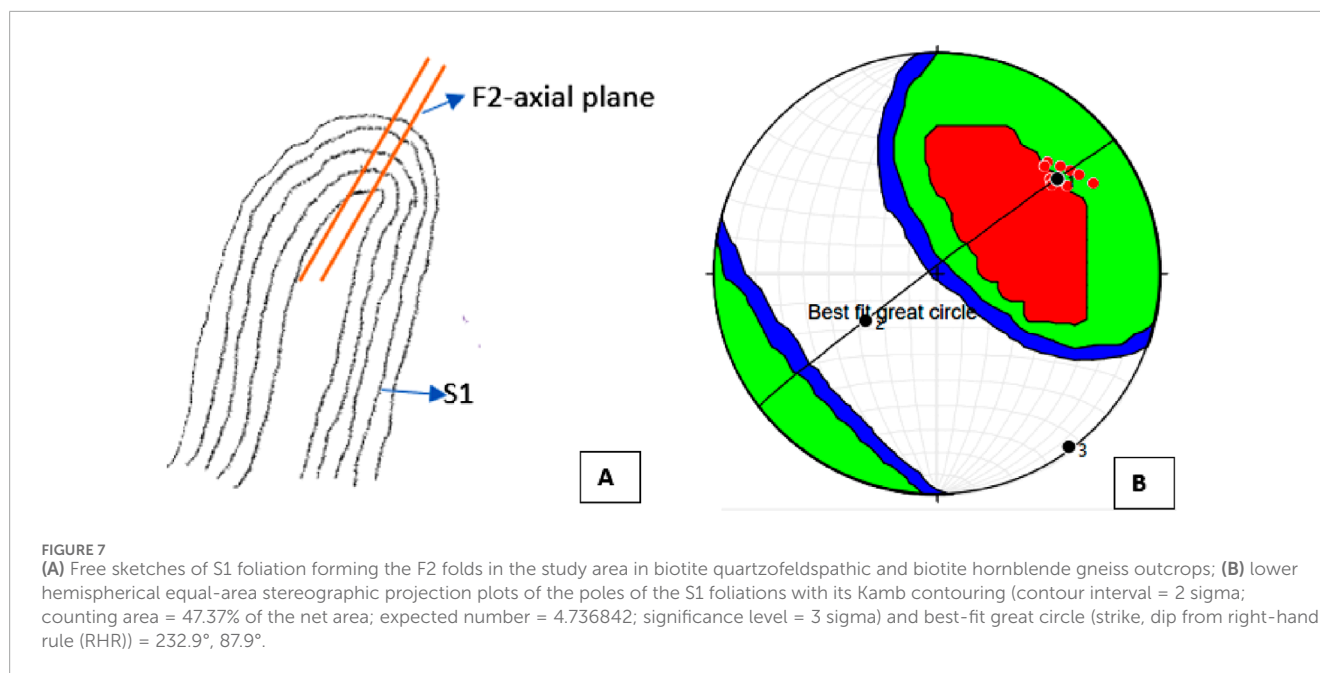
(A) Field photograph of the quartz-feldspathic migmatite outcrop. (B,C) Microphotographs of quartz-feldspathic migmatite. (D) Field photograph of amphibolite gneiss alteration (chloritization) resulting from the later retrograde metamorphism. (E,F) The microphotographs of amphibolite gneiss that show overgrowth of opaque mineral on amphibole grains. XPL = Q17 cross-polarized view, PPL = plane-polarized view.



**FIGURE 5** (A) Field and microphotograph of hornblende gneiss, whose rock unit is strongly foliated and shows vertical compositional banding cross-cut by quartz vein. (B, C) Microphotographs of hornblende gneisses in the cross-polarized view (XPL) and plane-polarized view (PPL), respectively. (D) Field photographs of biotite-hornblende gneiss showing the gneissic banding structure and high shearing effect. (E, F) Microphotographs of the biotite-hornblende gneiss in cross-polarized view (XPL) and plane-polarized view (PPL), respectively.



**FIGURE 6** (A) Field photograph of the biotite quartzofeldspathic gneiss cut by two perpendicular quartz veins; (B, C) microphotographs of the biotite quartzofeldspathic gneiss showing the crystallization of biotite grains in cross-polarized view (XPL) and plane-polarized view (PPL), respectively. (D) Field photographs of the granitic gneiss; (E, F) microphotographs of the granitic gneiss showing recrystallization of quartz grains in the cross-polarized view (XPL) and plane-polarized view (PPL), respectively.



quartz (up to 38%), plagioclase (up to 15%), biotite (up to 3%), and opaques (about 1%), with apatite, sphene, and zircon occurring as accessory minerals (Figures 6E,F). Alteration of biotite to traces of chlorite and muscovite is observed, and sericitization of feldspars is also common. The foliation is defined by elongation of quartz and feldspars that occurs by the alignment of biotites. Most of the quartz grains show undulate extinction and are anhedral; the granular and perthitic texture is also common.

## 5.2 Structural and deformation history of the Gida Ayana area

The structural and deformation history of the study area was analyzed based on detailed field investigations of the overprinting and cross-cutting relationships as well as petrographic studies of metamorphic rocks from thin sections. The rock geometries and their attitudes in the field as well as petrographic analysis on the study area revealed that the rocks of the Gida Ayana area have a polyphased deformation history. Thus, the study area has at least three ductile deformation phases (D1 to D3) and brittle structures like irregular fractures, joints, and veins. Each structure observed in the study area and its deformation history are discussed in detail below.

### 5.2.1 Early deformation structures (D1 phase)

The D1 phase is recognized as the early deformation event in the Gida Ayana area, which resulted in only S1 foliations. There are no visible fold structures related to the observed D1 events, but alternate layers of light and pink-colored quartz and feldspar minerals as well as mafic- and felsic-rich gneisses and metamorphic bands form the first S1 foliations parallel to the axial plane of the interfacial F2 fold (Figures 7A, 8A). The S1 foliation has a northwest trend with moderate-to-steep dipping to the west or east (Figure 7B). The S1 foliation is a local penetrative foliation that is weaker in the coarse-grained quartzofeldspathic rocks.

### 5.2.2 Secondary deformation structures (D2 phase)

The structural elements of the second phase of deformation in the study area are the products of east–west non-coaxial shortening events and form the major fabric in the area. The D2 deformations produced F2 folding, S2 foliations, and L2 lineations, as identified in the area. Thus, the D2 event was probably caused by a north–northeast to south–southwest directed progressive compression owing to plate convergence, which developed the following structures.

#### 5.2.2.1 S2 foliations

The S2 foliations are the major structural elements in the study area. Megascopically, these are defined by gneissic banding and alignment of minerals like quartz and feldspars. They are crosscut by pegmatite veins, aplitic dikes, and local shear dextral porphyroblasts within the main foliation fabric. The S2 foliations are generally oriented in the northeast–southwest direction with a southern dip (Figure 9A) and are uniformly developed over the entire Precambrian units of the study area. However, the quartz-feldspar migmatite unit has undergone a prolonged period of migmatization and is highly intruded upon by veins; hence, the general continuity of the S2 foliations is highly disrupted.

#### 5.2.2.2 F2 folds

The early S1 surface folds to produce the F2 fold, which is the first kind of fold caused by the D2 deformation event and is localized at the mesoscopic scale. East of the Kile River, the sheared quartz-feldspar gneiss is commonly exposed and represents the F2 mesoscopic fold, which is upright and sub-horizontal in the biotite quartz-feldspar gneiss with a fold axis plunging approximately 27° and vertical axial plane with an average tendency of 30° (Figure 9B). The F2 folds are abundant and rather tight within the quartz-feldspar migmatite, but their exposure is rare because of migmatization.

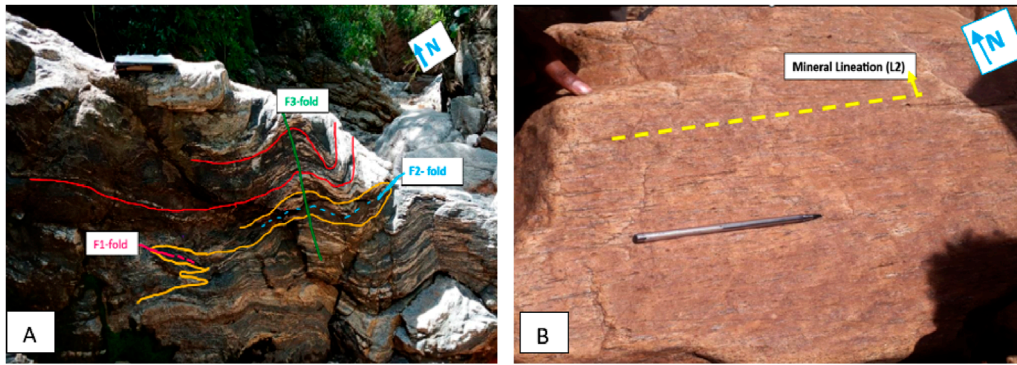


**FIGURE 8** (A) Field photographs of different types of mesoscopic folds with different generations based on overprinting relationship and cross-cutting principal biotite quartzofeldspathic gneiss outcrop; (B) stretched mineral lineation (L2) in the granitic gneiss.

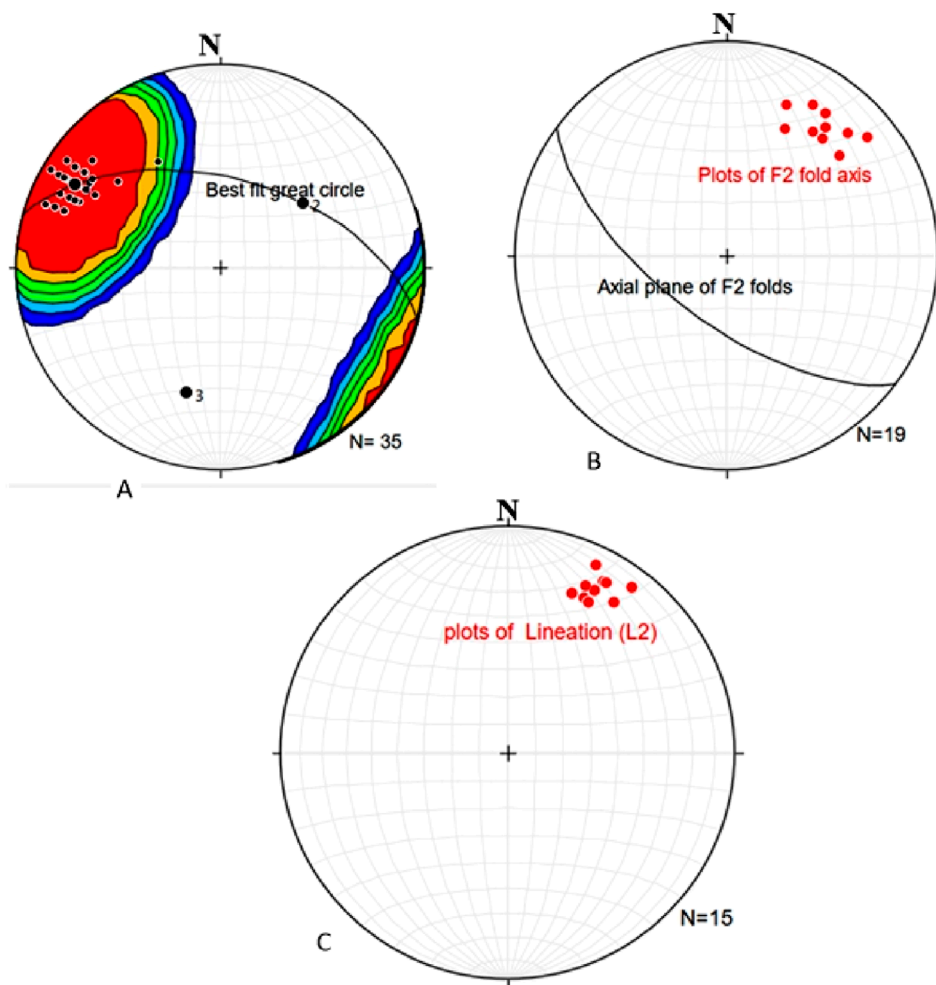


**FIGURE 9** (A) Lower hemispherical equal-area stereographic projection plot of the poles of the S2 foliations with its Kamb contouring (contour interval = 2 sigma; counting area = 22.5% of the net area; expected number = 6.975; significance level = 3 sigma) and best-fit great circle (strike, dip from RHR) = 284.8°, 53.8°. (B) Lower hemispherical equal-area stereographic projection plot of the F2 fold axis with its average axial plane (strike, dip = 126.6°, 64.6° S) and interlimb angle of 25.8°. (C) Lower hemispherical equal-area stereographic projection plot of the mineral lineations L2 in the study area.

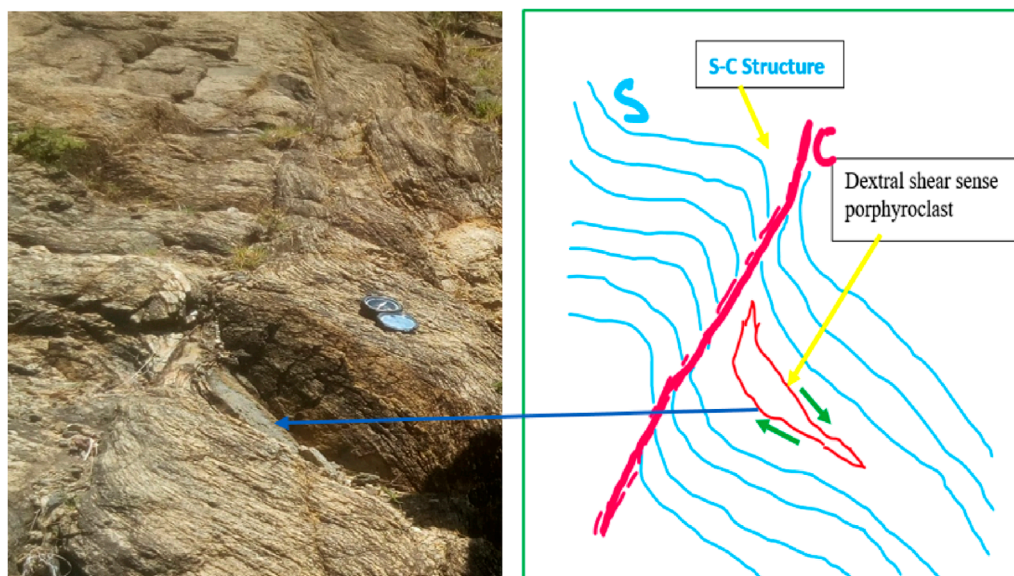


**FIGURE 10**  
Field photographs of S-C structures with local dextral shear-sense porphyroblasts and their sketch in the biotite-hornblende gneiss outcrop.

The F2 folding must have been produced by the high intensity of shortening stress as the folds are intrafolial and have a very narrow interlimb angle.

### 5.2.2.3 L2 lineations

These are sub-horizontal mineral aggregate lineations defined by felsic minerals (quartz and feldspar) that plunge in the near-northeast orientation with a mean plunge of  $15^{\circ}$ – $30^{\circ}$  (Figures 8B, 9C). Mineral lineations defined by mafic minerals (biotite or amphibole) are also observed in the more schistose rocks. Lineations formed by the F2 fold axes are also observed at different locations.

## 5.2.3 Late deformation structures (D3 phase)

### 5.2.3.1 S3 foliations

These foliations are caused by the parallel arrangement of certain mineral grains that give the rock a lined appearance and are formed when the pressure squeezes the flat or elongated minerals within a rock. They are characterized by planar arrangement of the structural features parallel to the axial plane of the F3 fold and ductile shear zone in the rock (Figure 10). S3 foliations, particularly those resulting from the alignment of constituent mineral grains, are observed in all lithological units but mainly in the amphibole, hornblende, biotite–hornblende, and biotite quartz–feldspar gneisses owing to the realignment of minerals when subjected to high pressures and temperatures. The orientations of the S-C structures and ductile shear zone are north–northeast to south–southwest with easterly dipping that cross-cut the previous S1 and S2 foliations (Figure 11A).

### 5.2.3.2 F3 folds

Mesoscopic shear-related F3 folds are asymmetric Z-folds observed in the field (Figure 8A). A stereographic plot of the F3 fold axes is shown in Figure 11B. These structures develop by folding of

the S3 foliations. Additionally, quartz and pegmatite veins are also folded to form this type of fold.

## 5.2.4 Brittle structures

### 5.2.4.1 Joints

Joints are a type of brittle structural fractures identified in the metamorphic rocks of the study area that have variable opening style and geometry (Figures 12A, B). The joints observed in the study area are mostly northwest–southeast trending with sub-vertical to vertical dipping (Figure 13). These structures are formed as a result of later deformations. Some of the joints and fractures observed in the field are also filled by quartz or calcite veins.

### 5.2.4.2 Veins

Different exposed veined structures were noted in the study area; these included both syntaxial (Figure 14A) and antitaxial (Figure 14B) vein types based on the petrographic analysis. The most common veins in the study area were calcite and quartz, and both were observed in the metavolcanic and metasedimentary rocks of the study area at the mesoscopic or microscopic scale.

## 5.3 Metamorphism

According to Miyashiro (1994), metamorphism is a collective term for the mineralogical, chemical, and textural changes occurring in rocks in an almost solid state (i.e., without substantial melting) in the deeper parts of the Earth at temperatures higher than those on the Earth's surface. It is typically associated with elevated temperature and pressure and therefore affects rocks within the Earth's crust and mantle (Bucher and Grapes, 2011). Metamorphism, metamorphic processes, and mineral transformations occurring in rocks at elevated temperatures and pressures are fundamentally

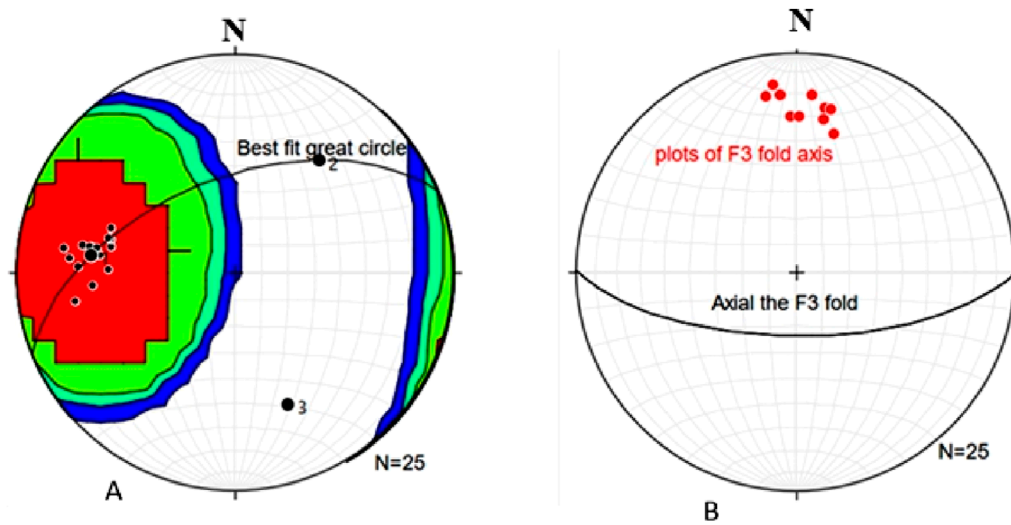


FIGURE 11

(A) Lower hemispherical equal-area stereographic projection plot of the poles of the shear zone (S3 foliation) with its Kamb contouring (contour interval = 2 sigma; counting area = 37.5% of the net area; expected number = 5.625; significance level = 3 sigma) and best-fit great circle (strike, dip from RHR) = 248.0°, 54.7°. (B) Lower hemispherical equal-area stereographic projection plot of the F3 fold axis with its average axial plane (strike, dip = 90.3°, 66.3° S) and interlimb angle of 20.9°.

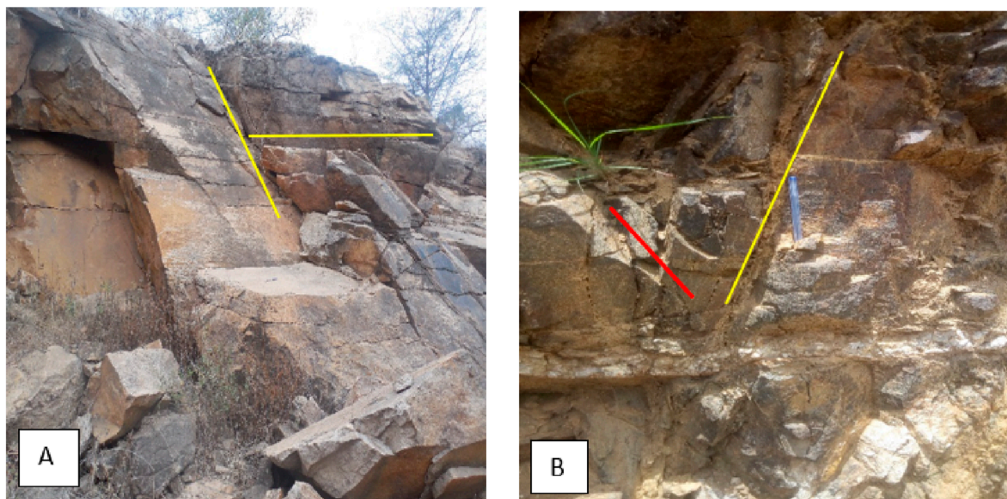


FIGURE 12

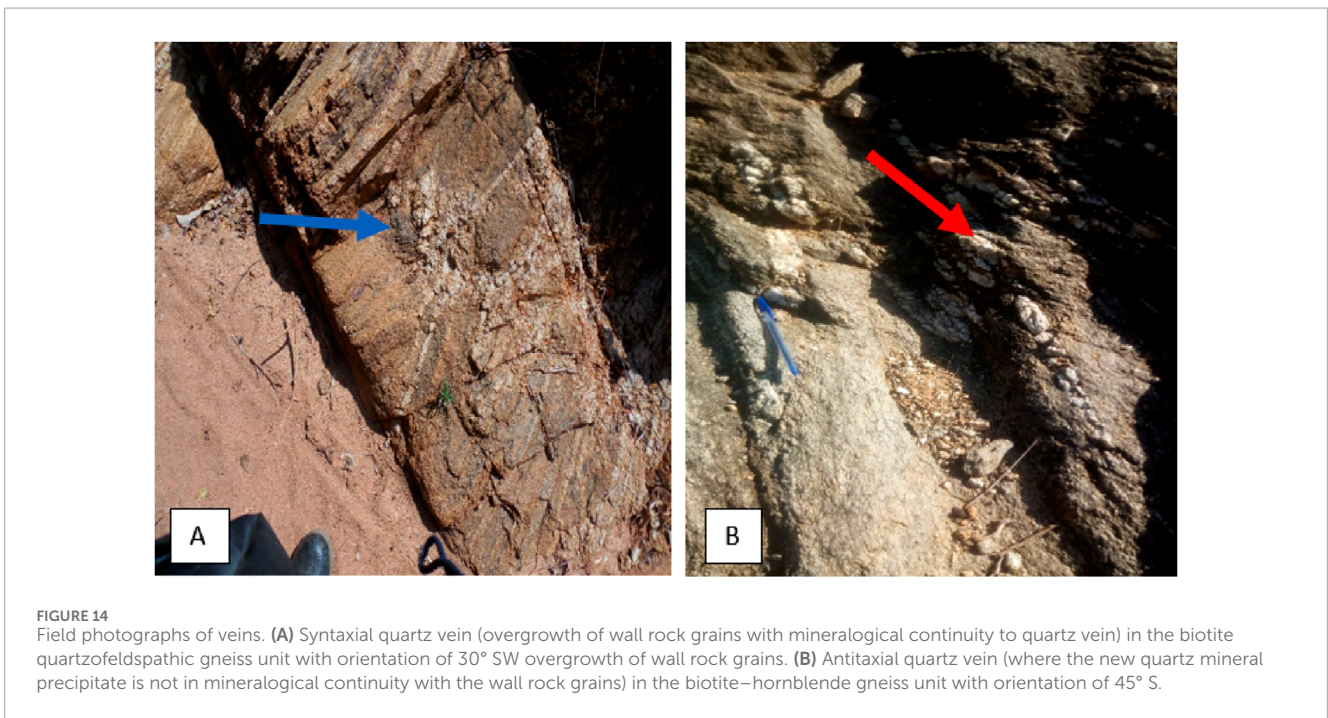
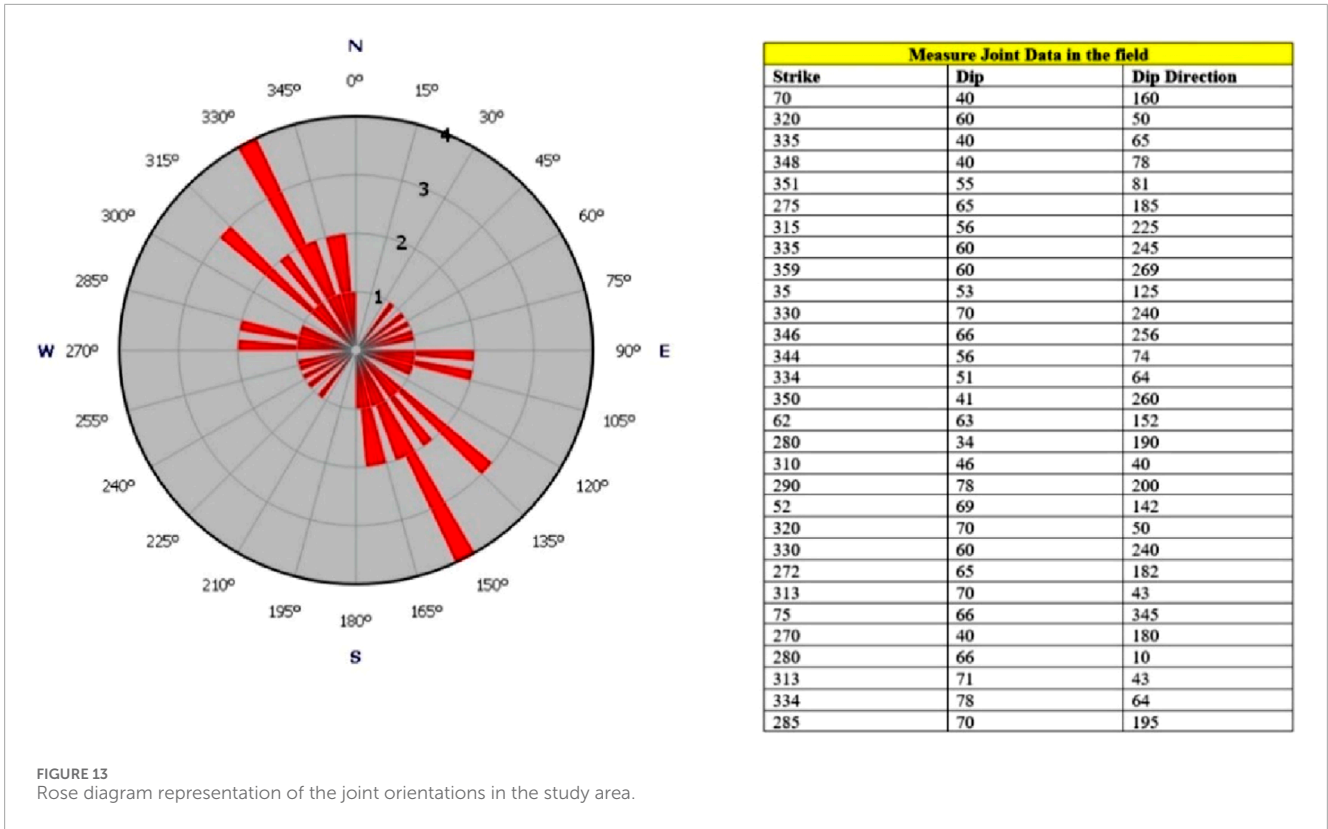
Field pictures of different orientations of joints in the Gida Ayana rocks. (A) Field photographs of two sets of joints in the granitic gneiss. (B) Three sets of joints in the biotite quartzofeldspathic gneiss.

associated with chemical reactions. These changes are collectively known as metamorphic crystallization, which leads to the formation of appropriate equilibrium mineral assemblages under appropriate conditions when such conditions persist over a long period of time. The mineral assemblage depends on the bulk chemical composition of the rock and physical conditions of metamorphism (Spry, 2011). Following the tectonothermal event that affected the EAO during the Neoproterozoic to early Cambrian and based on field study as well as petrographic analysis, all the rocks in the Gida Ayana area of western Ethiopia were found to have experienced various deformations and metamorphic mineral growths at the mesoscopic and microscopic scales. These mesoscopic- and microscopic-scale studies of the 23

representative samples selected in this work reveal that various deformational phases and mineralogical assemblage changes had occurred in the area. The modal abundances of the mineralogical assemblages, degrees of deformation, alterations, and presence of index minerals were studied under a petrographic microscope. As a result, at least two metamorphism phases were recognized to be associated with the deformation phases of the area. The mineral assemblages of various rock units from the study area are as follows.

### 5.3.1 Quartz–feldspar migmatite

The metamorphic mineral assemblages of most of the studied samples in the area consisted of orthoclase + plagioclase +



microcline + quartz + hornblende ± apatite, while the alteration products included biotite + muscovite + chlorite ± epidote. The minerals are typically characterized by coarse-grained dimensions and preferred orientations defining the regional S2 fabric. The low-grade minerals (muscovite, biotite, and chlorite) grow along with the narrow shear bands or near the shear zones. The assemblage

orthoclase + plagioclase + microcline + quartz ± hornblende indicates that this rock is metamorphosed to medium-to-high grade with upper amphibolite facies condition of metamorphism. The coarse-grained granoblastic texture along with coexistence of hornblende and calcic plagioclase may indicate an amphibolite facies, and the migmatization of the rock constrains the temperature

to over 700°C (above wet granite melt). This assemblage is regarded as prograde metamorphism (M1) from the parental rock. The alteration products muscovite + chlorite ± biotite + epidote ± albite are indicative of hydration reactions that may have occurred during uplift or in the D3 shearing zone related to fluid migration. This marks the low-grade greenschist facies and the second or retrograde metamorphic event (M2) in the area.

### 5.3.2 Biotite quartz–feldspar gneiss unit

The biotite quartz–feldspar gneiss unit shows two slightly different metamorphisms and mineralogical assemblages compared to the quartz–feldspar migmatite, with lesser amount of mafic minerals such as hornblende. These assemblages represent two phases of metamorphism (M1 and M2). Orthoclase + plagioclase + quartz + biotite ± sphene is the mineral assemblage indicating prograde metamorphism, whereas chlorite + muscovite ± biotite ± epidote is the mineral assemblage representing retrograde metamorphism in this unit. The mineral assemblage orthoclase + plagioclase + quartz + biotite ± sphene is characterized by coarse-grained and well-developed granoblastic texture with clear bimodal grain size distribution in more sheared rocks. This mineral assemblage is characterized by dimensional preferred orientations defining the major S1 and S2 fabrics.

Generally, the low-grade minerals (muscovite, chlorite, epidote, and biotite) grow along the narrow shear zones. The mineral assemblage orthoclase + plagioclase + quartz ± sphene indicates high-grade metamorphic rocks with upper amphibolite facies. The existence of the coarse-grained texture of orthoclase, calcic plagioclase, and disappearance of anhydrous minerals (pyroxene) indicate that this rock unit is characterized by the upper amphibolite facies metamorphism. The alteration products sericitic muscovite, chlorite, and biotite are indicative of retrograde metamorphism that may have occurred during uplift or D3-shear-zone-related fluid migrations.

### 5.3.3 Mafic (amphibole, hornblende, and biotite–hornblende) gneisses

Mafic gneisses are widely exposed in the study area and are highly prone to weathering as they are largely composed of mafic minerals like biotite and hornblende. The samples representing these units from the study area were collected, and their thin sections were prepared and analyzed using a petrographic microscope. The metamorphism in this unit shows two phases, namely M1 and M2. The unit is composed of hornblende, feldspar, pyroxene, biotite, and quartz along with alteration features such as chlorination and epidotization resulting from later retrograde metamorphism.

Biotite + hornblende + plagioclase + clinopyroxene + orthoclase + quartz is the mineral assemblage for the prograde metamorphism indicating the upper amphibolite facies metamorphism, while epidote ± chlorite ± muscovite ± apatite + opaque minerals define the mineral assemblage for the retrograde metamorphism. The hornblende grains are highly altered to epidote and chlorites; these grains are usually very coarse, as observed under the microscope. Biotite appears platy and exists in equilibrium conditions with hornblende. The plagioclase grains are coarse and are usually calcic (andesine) subhedral to anhedral in shape, with slight alteration to sericite in some places. The main assemblage of hornblende + biotite + plagioclase + clinopyroxene + orthoclase + quartz indicates that this rock is also metamorphosed to medium-to-high grade with

upper amphibolite facies condition of metamorphism. The coarse-grained granoblastic texture as well as coexistence of hornblende and calcic plagioclase may further indicate the upper amphibolite facies metamorphism.

### 5.3.4 Granitic gneiss

This gneissic unit also shows two slightly different mineralogical assemblages compared to the other metamorphic rock units. It has a small amount of mafic minerals such as biotite and hornblende. The assemblages represent the two phases of metamorphism (M1 and M2); orthoclase + plagioclase + microcline + quartz ± sphene + opaque minerals constitute the mineral assemblage for prograde metamorphism, while chlorite + muscovite ± biotite ± epidote represents the mineral assemblage for the retrograde metamorphism in this unit.

## 5.4 Temporal relationship between metamorphic mineral growth and deformation

Understanding the relationships between metamorphic mineral growth and deformation provides a more comprehensive understanding of the tectonic and metamorphic history of the Gida Ayana area. Metamorphic mineral growth is highly influenced by the deformation processes in the study area. In regions subjected to tectonic forces, deformations (such as shearing and folding) can facilitate the nucleation, growth, and changes of specific metamorphic minerals, such as sillimanite, garnet, biotite, and andalusite, depending on the grade of metamorphism. The textural evidence in metamorphic rocks provides critical clues about the timing of mineral growth in relation to deformation. Several key aspects are considered for the interpretations, such as deformed and undeformed mineral textures, porphyroblast growth, synchronous deformation, and mineral growth. The development of foliation and lineation is often a direct result of both deformation and mineral growth. Minerals like mica, chlorite, and quartz tend to align during deformation, forming foliated structures that are oriented parallel to the principal strain directions. As described in the discussion, the structures and deformation history of the study area are affected by three phases of ductile deformations and associated brittle deformation. Moreover, the metamorphic mineral assemblages and related microstructures are as described earlier. Although no distinct porphyroblast growth was observed, the textural and fabric relationships indicate that the timings of the peak and retrograde metamorphisms are related to two major deformation phases, as summarized in [Table 2](#). The major dimensional alignment of metamorphic minerals is generally parallel to the S1–S2 gneissic banding, which allows reaching M1 during D2 deformation. The retrograde minerals define the D3 shear fabric (S3 surface) and represent the M2 phase of metamorphism. M1 is a prograde event that may have evolved from D1 to D2 deformation. The alteration products chlorite, muscovite, epidote, and biotite are indicative of hydration reactions that may have occurred during uplift or D3-shear-zone-related fluid migrations.

TABLE 2 Summary of the metamorphic mineral growths with respect to deformation phases.

Metamorphic minerals	Phases of deformation		
	Pre D2	Syn D2	Syn D3
Quartz	—————		
Plagioclase	—————		
Orthoclase	— ■ — ■ ■	—————	
Hornblende	— ■ ■	—————	—————
Biotite	—————		
Chlorite			—————
Epidote			—————
Muscovite			—————
Condition of metamorphism	Middle amphibolite	Upper amphibolite	Greenschist

Note: Metamorphic events (M1 = first phase of metamorphism, M2 = second phase of metamorphism); deformation events (Pre D2 = deformation before D2, Syn D2 = deformation during the second phase of deformation, Syn D3 = deformation during the third phase of deformation).

## 6 Conclusion

The geological study of Ethiopia's basement rocks from the Gida Ayana area reveals significant findings regarding petrography, metamorphism, and deformation history. Through detailed fieldwork involving geological mapping, rock sample collection, and detailed observations, we analyzed the petrography and metamorphism of the rocks thoroughly. Our analyses reveal the complex mineral compositions, metamorphic grades, and deformation history of the Precambrian rocks in the Gida Ayana district. The integration of petrographic, metamorphic, and deformation data facilitated reconstruction of the geological history of the basement rocks by shedding light on their significance in the context of regional tectonic evolution. The findings of this study not only enhance our understanding of the Gida Ayana rocks but also pave the path for potential future research efforts in this area, contributing to broader geological knowledge. The study area is part of the high-grade metamorphic terrane of the WES that is dominated by both high-grade metamorphic and intrusive rocks. The rock types in the study area include quartz-feldspar migmatite, amphibole gneiss, hornblende gneiss, biotite-hornblende gneiss, quartzofeldspathic gneiss, and granitic gneiss. These rocks exhibit various mineral compositions, textures, and structural features indicative of their metamorphic histories. The presence of secondary structures like joints, fractures, and quartz veins further adds to the geological complexity of the area. Petrographic analyses reveal the mineralogical composition of each rock unit and shed light on their formation and alteration history.

The structural and deformation history of the Gida Ayana area was thoroughly analyzed through detailed field investigations, overprinting, and cross-cutting relationships as well as petrographic studies of metamorphic rocks from thin sections. The findings reveal a complex polyphase deformation history with at least three ductile deformation phases (D1 to D3) and development

of brittle structures, such as irregular fractures, joints, and veins. Each structure observed in the study area, including the early (D1), secondary (D2), and late (D3) deformation events, were discussed in detail to highlight the formation of F2 folds, S2 foliations, L2 lineations, S3 foliations, F3 folds, joints, and veins. The orientations, characteristics, and implications of these structures were methodically examined to provide valuable insights into the geological evolution of the Gida Ayana area.

The study area has undergone significant metamorphic processes, resulting in the formation of distinct mineral assemblages in different rock units. Metamorphism driven by elevated temperatures and pressures has led to the development of prograde and retrograde mineral phases, indicating two metamorphic events (M1 and M2) in the area. The temporal relationships between metamorphic mineral growth and deformation reveal that the major dimensional alignment of the metamorphic minerals corresponds to specific phases of ductile deformation (D1 to D3). The presence of hydration reactions and alteration products, such as chlorite, muscovite, epidote, and biotite, further indicate the influences of fluid migrations during the metamorphic processes. Overall, the findings provide valuable insights into the tectonothermal history of the EAO and contribute to our understanding of the metamorphic processes in this region. Moreover, the study area is a part of the high-grade metamorphic terrane of the WES dominated by high-grade metamorphic rocks, which are represented by the orthogneiss Gore-Gambella (Ayalew and Peccerillo, 1998). These deformation and metamorphic phases are thought to have occurred during the continent-to-continent convergence and eventual collision phase of east Africa (Stern, 1994). We therefore suggest that future research efforts should involve establishing a multidisciplinary project combining structural geology, geochemistry, geochronology, and geophysics to create a detailed high-resolution tectonic and metamorphic map of the Gida Ayana region. This would include geochronological sampling (e.g., U-Pb zircon dating) to establish

a clear timeline of the tectonometamorphic events, petrographic and geochemical analyses to map the metamorphic facies and mineralization patterns, and use of geophysical techniques (e.g., magnetometry or resistivity surveys) to explore subsurface structures and relationships between the surface features and deeper geological formations. By addressing these specific areas, future research could significantly advance our understanding of the tectonometamorphic evolution of the EAO and its implications for regional geology and tectonics.

## Data availability statement

The original contributions presented in the study are included in the article/supplementary material, and any further inquiries may be directed to the corresponding author.

## Author contributions

BM: conceptualization, data curation, formal analysis, funding acquisition, investigation, methodology, project administration, resources, software, supervision, validation, visualization, writing – original draft, and writing – review and editing. AW: conceptualization, data curation, formal analysis, funding acquisition, investigation, methodology, project administration, resources, software, supervision, validation, visualization, writing – original draft, and writing – review and editing.

## Funding

The author(s) declare that no financial support was received for the research and/or publication of this article.

## References

- Abbate, E., Bruni, P., and Sagri, M. (2015). Geology of Ethiopia: a review and geomorphological perspectives. *World Geomorphol. Landscapes*, 33–64. doi:10.1007/978-94-017-8026-1\_2
- Abdelsalam, M., and Stern, R. (1996). Sutures and shear zones in the arabian-nubian shield. *J. Afr. Earth Sci.* 23 (3), 289–310. doi:10.1016/s0899-5362(97)00003-1
- Alemu and Abebe (2007). Geology and tectonic evolution of the pan-african Tulu Dimtu belt, western Ethiopia. *Online J. Earth Sci.* 1, 24–42. Available online at: <https://www.researchgate.net/publication/32384685>.
- Allen, A., and Tadesse, G. (2003). Geological setting and tectonic subdivision of the Neoproterozoic orogenic belt of Tuludimtu, western Ethiopia. *J. Afr. Earth Sci.* 36 (4), 329–343. doi:10.1016/s0899-5362(03)00045-9
- Allen, A., and Tadesse, G. (2005). Reply to discussion of “geological setting and tectonic subdivision of the neoproterozoic orogenic belt of tuludimtu, western Ethiopia” [A. Allen, G. Tadesse, *Journal of African Earth Sciences* 36 (2003) 329–343]. *J. Afr. Earth Sci.* 41 (4), 333–336. doi:10.1016/j.jafrearsci.2005.05.005
- Asrat, A., and Barbey, P. (2003). Petrology, geochronology and Sr-Nd isotopic geochemistry of the Konso pluton, south-western Ethiopia: implications for transition from convergence to extension in the Mozambique Belt. *Int. J. Earth Sci.* 92 (6), 873–890. doi:10.1007/s00531-003-0360-9
- Asrat, Barbey, P., and Gleizes, G. (2001). Precambrian geology of Ethiopia: a review. *Afr. Geosci. Rev.* 8 (3), 271–288. Available online at: <https://www.researchgate.net/publication/313679396>.
- Avigad, D., Stern, R., Beyth, M., Miller, N., and McWilliams, M. (2007). Detrital zircon U–Pb geochronology of cryogenian diamictites and lower paleozoic sandstone in Ethiopia (tigray): age constraints on neoproterozoic glaciation and crustal evolution of the southern arabian–nubian shield. *Precambrian Res.* 154 (1–2), 88–106. doi:10.1016/j.precamres.2006.12.004
- Ayalew, T. (1997). Metamorphic and structural evolution of the Gore-Gambella area, Western Ethiopia. *Ethiop. J. Sci.* 20 (2). doi:10.4314/sinet.v20i2.18103
- Ayalew, T., Bell, K., Moore, J. M., and Parrish, R. R. (1990). U–Pb and Rb–Sr geochronology of the western Ethiopian shield. *Geol. Soc. Am. Bull.* 102 (9), 1309–1316. doi:10.1130/0016-7606(1990)102
- Ayalew, T., and Johnson, T. E. (2002). The geotectonic evolution of the Western Ethiopian shield. *SINET Ethiop. J. Sci.* 25 (2). doi:10.4314/sinet.v25i2.18082
- Ayalew, T., and Peccerillo, A. (1998). Petrology and geochemistry of the Gore-Gambella plutonic rocks: implications for magma genesis and the tectonic setting of the Pan-African Orogenic Belt of western Ethiopia. *J. Afr. Earth Sci.* 27 (3–4), 397–416. doi:10.1016/s0899-5362(98)00070-0
- Blades, M. L. B., Collins, A. S., Foden, J., Payne, J. L., Xu, X., Alemu, T., et al. (2015). Age and hafnium isotopic evolution of the Didesa and Kemashi Domains, western Ethiopia. *Precambrian Res.* 270, 267–284. doi:10.1016/j.precamres.2015.09.018
- Berhe, S. M. (1990). Ophiolites in northeast and east Africa: implications for proterozoic crustal growth. *J. Geol. Soc.* 147 (1), 41–57. doi:10.1144/gsjgs.147.1.0041
- Braathen, A., Grenne, T., Selassie, M., and Worku, T. (2001). Juxtaposition of neoproterozoic units along the baruda–tulu Dimtu shear-belt in the East african orogen of western Ethiopia. *Precambrian Res.* 107 (3–4), 215–234. doi:10.1016/s0301-9268(00)00143-1

## Acknowledgments

The authors would like to acknowledge the Ethiopian Institute of Geological Survey for access to the preparation of thin sections of rock samples. The authors also express their deepest thanks to the Gida Ayana Woreda Administrative and mine development office, Gida Ayana town administrative office and communities, and the residents of the area for their respectful acceptance and advice during field work.

## Conflict of interest

The authors declare that the research was conducted in the absence of any commercial or financial relationships that could be construed as a potential conflict of interest.

## Generative AI statement

The authors declare that no Generative AI was used in the creation of this manuscript.

## Publisher's note

All claims expressed in this article are solely those of the authors and do not necessarily represent those of their affiliated organizations, or those of the publisher, the editors and the reviewers. Any product that may be evaluated in this article, or claim that may be made by its manufacturer, is not guaranteed or endorsed by the publisher.

- Bucher, K., and Grapes, R. (2011). *Petrogenesis of metamorphic rocks*. 8th ed. 2011 ed. Springer.
- Gani, N. D., and Abdelsalam, M. G. (2006). Remote sensing analysis of the gorge of the Nile, Ethiopia with emphasis on Dejen–Gohatsion region. *J. Afr. Earth Sci.* 44 (2), 135–150. doi:10.1016/j.jafrearsci.2005.10.007
- Grenne, T., Braathen, A., Gebreselassie, M., and Worku, T. (1998). Results and models from fieldwork in the Meso-Neoproterozoic belt of western Ethiopia: the Wember Baruda-Bulen-Kilaj transect of the Metekel zone. *Norges Geol. Undersøkelse Rep.* 98.
- Johnson, P. R., and Woldehaimanot, B. (2003). Development of the Arabian-Nubian shield: perspectives on accretion and deformation in the northern East African orogen and the assembly of Gondwana. *Geol. Soc. Lond. Spec. Publ.* 206 (1), 289–325. doi:10.1144/gsl.sp.2003.206.01.15
- Johnson, T. E., Ayalew, T., Mogessie, A., Kruger, F., and Poujol, M. (2004). Constraints on the tectonometamorphic evolution of the western Ethiopian shield. *Precambrian Res.* 133 (3–4), 305–327. doi:10.1016/j.precamres.2004.05.007
- Kazmin, V., Shifferaw, A., and Balcha, T. (1978). The Ethiopian basement: stratigraphy and possible manner of evolution. *Geol. Rund* 67 (2), 531–546. doi:10.1007/bf01802803
- Kebede, T., and Koeberl, C. (2003). Petrogenesis of A-type granitoids from the Wallagga area, western Ethiopia: constraints from mineralogy, bulk-rock chemistry, Nd and Sr isotopic compositions. *Precambrian Res.* 121 (1–2), 1–24. doi:10.1016/s0301-9268(02)00198-5
- Kroner, A., and Stern, R. J. (2004). AFRICA | pan-african Orogeny. *Encycl. Geol.* 1, 1–12. doi:10.1016/B0-12-369396-9/00431-7
- Kusky, T. M., Abdelsalam, M., Stern, R. J., and Tucker, R. D. (2003). Preface: evolution of the East African and related orogens, and the assembly of Gondwana. *Precambrian Res.* 123, 81–85. doi:10.1016/s0301-9268(03)00062-7
- Li, Z., Bogdanova, S., Collins, A., Davidson, A., De Waele, B., Ernst, R., et al. (2008). Assembly, configuration, and break-up history of Rodinia: a synthesis. *Precambrian Res.* 160 (1–2), 179–210. doi:10.1016/j.precamres.2007.04.021
- Miyashiro, A. (1994). *Metamorphic petrology*, 131. London: UCL Press, 710–710p.
- Spry, A. (2011). *Metamorphic textures*. 2nd ed. Oxford, London: Pergamon Press, 350pp.
- Stern, R. (1994). Arc assembly and continental collision in the Neoproterozoic East African orogen: implications for the consolidation of Gondwanaland. *Annu. Rev. Earth Planet. Sci.* 22, 319–351. doi:10.1146/annurev.ea.22.050194.001535
- Stern, R., Ali, K. A., Abdelsalam, M. G., Wilde, S. A., and Zhou, Q. (2012). U–Pb zircon geochronology of the eastern part of the Southern Ethiopian Shield. *Precambrian Res.* 206–207, 159–167. doi:10.1016/j.precamres.2012.02.008
- Tefera, T. C., and Haro, W. (1996). *Explanation of the geological map of Ethiopia*. Addis Ababa, Ethiopia: Ethiopian Institute of Geological Surveys.
- Tsigie, L., and Abdelsalam, M. (2005). Neoproterozoic–early Paleozoic gravitational tectonic collapse in the southern part of the Arabian-Nubian shield: the Bulbul belt of southern Ethiopia. *Precambrian Res.* 138 (3–4), 297–318. doi:10.1016/j.precamres.2005.05.005
- Yihunie, T., and Hailu, F. (2007). Possible eastward tectonic transport and northward gravitational tectonic collapse in the Arabian–Nubian shield of western Ethiopia. *J. Afr. Earth Sci.* 49 (1–2), 1–11. doi:10.1016/j.jafrearsci.2007.04.006